

# Electrostatic Grating of Nanorods

Angelos Kamariadis

School of Electrical and Computer Engineering

National Technical University of Athens

Athens, Greece

angeloskamariadis@gmail.com

**Abstract**—This paper investigates the electrostatic field and potential distribution within an infinite, one-dimensional periodic array of dielectric nanorods subjected to a uniform transverse electric field. By applying rigorous boundary conditions and utilizing complex Laurent series expansions, closed-form analytical solutions for the scattered and internal potentials are derived using a dipole approximation. The model accounts for mutual coupling between adjacent cylinders through a geometric lattice sum factor that dictates the non-locality of the array. The analytical solutions are supported by graphical representations of the electric and potential fields across the  $xy$ -plane, evaluating the effects of varying dielectric permittivities, angles of field incidence, and inter-cylinder periodicities. Results indicate that the geometric packing density strictly controls inter-rod interactions; dense arrays exhibit significant field distortion and strong coupling, whereas sparse configurations smoothly revert to isolated cylinder behavior.

**Index Terms**—Boundary Value Problems, Dielectric Cylinders, Electrostatic Scattering, Nanorods.

## I. PROBLEM FORMULATION

Consider a cylinder of radius  $a$  with a dielectric constant  $\varepsilon > 1$ , with its axis parallel to the  $\hat{z}$ -axis. The applied field is given by:

$$E_{\text{back}} = E_0(\hat{x} \cos \theta + \hat{y} \sin \theta).$$

In the  $xy$ -plane, the potential outside and inside the cylinder is written in polar coordinates  $(r, \phi)$  around its center:

- Outside (vacuum): keeping only the  $m = 1$  harmonic (the only one excited by a homogeneous field):

$$V_{\text{out}}(r, \phi) = -E_0 r \cos(\phi - \theta) + A \frac{a^2}{r} \cos(\phi - \theta).$$

- Inside (material with permittivity  $\varepsilon$ ):

$$V_{\text{in}}(r, \phi) = Br \cos(\phi - \theta).$$

## II. BOUNDARY CONDITIONS AND SOLUTION

We impose boundary conditions at  $r = a$ :

- Continuity of potential:  $V_{\text{out}} = V_{\text{in}}$ ,
- Continuity of normal displacement field ( $\hat{n} \cdot D$ ):  
 $\varepsilon_0 \partial_r V_{\text{out}} = \varepsilon \varepsilon_0 \partial_r V_{\text{in}}$ .

Solving yields:

$$A = E_0 \frac{\varepsilon - 1}{\varepsilon + 1} \equiv \xi E_0 \quad \text{and} \quad B = -\frac{2}{\varepsilon + 1} E_0$$

Therefore, we have:

$$V_{\text{out}} = -E_0 r \cos(\phi - \theta) + \xi E_0 \frac{a^2}{r} \cos(\phi - \theta)$$

$$V_{\text{in}} = -\frac{2}{\varepsilon + 1} E_0 r \cos(\phi - \theta)$$

(using  $E = -\nabla V$ )

## III. FORM OF TOTAL SCATTERED ELECTROSTATIC POTENTIAL AND POTENTIAL INSIDE THE CYLINDER

The centers of the cylinders are located at  $(0, 2nb)$  with  $n \in \mathbb{Z}$ . For each cylinder, we define local polar coordinates  $(r_n, \phi_n)$ .

Assuming, based on the problem statement, that the presence of the other cylinders does not introduce higher azimuthal harmonics (we restrict our analysis to  $m = 1$  for each cylinder), the total scattered potential is written as a superposition of dipoles for each cylinder. This uses the same coefficients across the entire array, but with local coordinate angles:

$$V_{\text{scat}}(x, y) = \sum_{n \in \mathbb{Z}} \frac{a^2}{r_n} [A_x \cos \phi_n + A_y \sin \phi_n] \quad (1)$$

where  $\cos \phi_n = \frac{x}{r_n}$ ,  $\sin \phi_n = \frac{y - 2nb}{r_n}$ , and  $r_n = \sqrt{x^2 + (y - 2nb)^2}$ .

The internal potential within each cylinder remains linear. Therefore, for the reference cylinder (or any cylinder  $n$ ):

$$V_{\text{in}}^{(0)}(r, \phi) = B_x r \cos \phi + B_y r \sin \phi$$

↓

$$V_{\text{in}}^{(0)}(x, y) = B_x x + B_y y$$

## IV. LAURENT SERIES

We use the complex representation  $z = re^{i\phi} = x + iy$  and centers at  $z_n = i2nb$ .

For  $|z| < |z_n|$  the following holds:

$$\frac{1}{z - z_n} = -\frac{1}{z_n} \sum_{m=0}^{\infty} \left( \frac{z}{z_n} \right)^m$$

Taking the real and imaginary parts and noting that:

$$\frac{\cos \phi_n}{r_n} = \Re \left( \frac{1}{z - z_n} \right) \quad \text{and} \quad \frac{\sin \phi_n}{r_n} = \Im \left( \frac{1}{z - z_n} \right)$$

we arrive, for  $r < 2|n|b$ , at series of the form:

$$\frac{\cos \phi_n}{r_n} = \sum_{m=1}^{\infty} C_{m,n} r^{m-1} \cos(m\phi) + D_{m,n} r^{m-1} \sin(m\phi)$$

$$\frac{\sin \phi_n}{r_n} = \sum_{m=1}^{\infty} \tilde{C}_{m,n} r^{m-1} \cos(m\phi) + \tilde{D}_{m,n} r^{m-1} \sin(m\phi)$$

with coefficients  $C_{m,n}, D_{m,n} \propto (2|n|b)^{-(m+1)}$  and alternating signs due to  $\arg z_n = \pm\pi/2$ .

The Laurent representation  $\sim r^{-m}$  arises if we expand for  $r > 2|n|b$ .

Both forms are consistent and useful depending on the region of convergence; here we need the expansion for  $r < a < b$ .

## V. APPLICATION OF BOUNDARY CONDITIONS TO FIND THE UNIQUE SOLUTION

Due to periodicity, all cylinders share the same coefficients  $(A_x, A_y)$  outside and  $(B_x, B_y)$  inside. The presence of the rest changes the local field at the center of each cylinder:

- The x-component is reduced
- The y-component is enhanced

After summing the fields at the center with two symmetric neighbors per  $n$ , a closed form emerges with a known lattice sum:

$$S = 2a^2 \sum_{n=1}^{\infty} \frac{1}{(2nb)^2} = \frac{a^2 \pi^2}{b^2 12} \quad (2)$$

Setting  $\xi = \frac{\varepsilon-1}{\varepsilon+1}$  (and  $\xi \rightarrow 1$  for PEC) and writing  $E_{0x} = E_0 \cos \theta$  and  $E_{0y} = E_0 \sin \theta$ , the self-consistent system yields:

$$A_x = \frac{\xi}{1 + \xi S} E_{0x} \quad \text{and} \quad A_y = \frac{\xi}{1 - \xi S} E_{0y} \quad (3)$$

The internal potential in each cylinder is:

$$V_{\text{in}}^{(n)}(x, y) = B_x x + B_y (y - 2nb),$$

$$B_x = -\frac{2}{\varepsilon + 1} (E_{0x} - S A_x),$$

$$B_y = -\frac{2}{\varepsilon + 1} (E_{0y} + S A_y)$$

The total potential at any point  $(x, y)$  (excluding the interior of a specific cylinder) is:

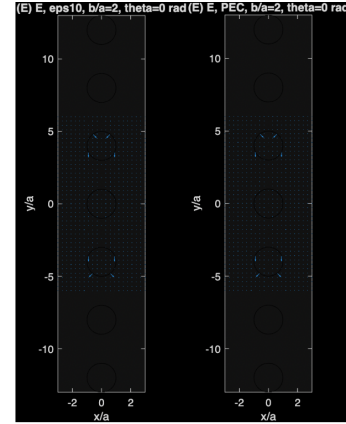
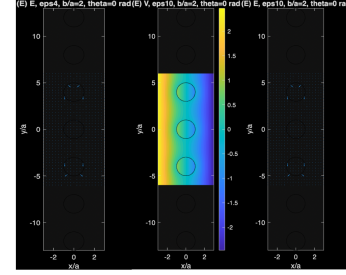
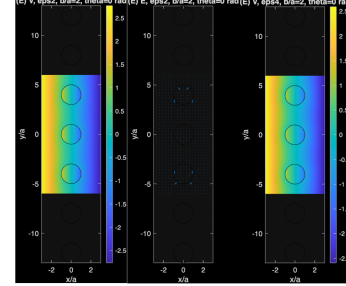
$$V(x, y) = -E_{0x}x - E_{0y}y + \sum_{n \in \mathbb{Z}} a^2 \left[ A_x \frac{x}{r_n^2} + A_y \frac{y - 2nb}{r_n^2} \right] \quad (4)$$

$$r_n^2 = x^2 + (y - 2nb)^2$$

while inside a cylinder, we replace the  $n$ -th term with the linear  $V_{\text{in}}^{(n)}$  for smoothness and application of the interface conditions. The field is  $E = -\nabla V$ . The above solution satisfies the boundary conditions (continuity of  $V$  and  $\hat{n} \cdot D$ ) under the assumption  $m = 1$ .

## VI. PLOTTING OF THE ELECTRIC AND POTENTIAL FIELDS IN THE X-Y PLANE (1)

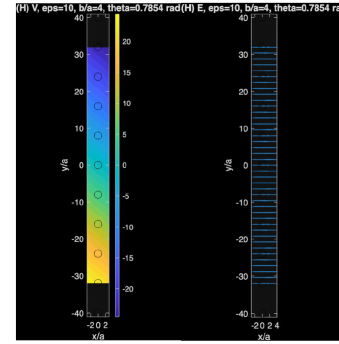
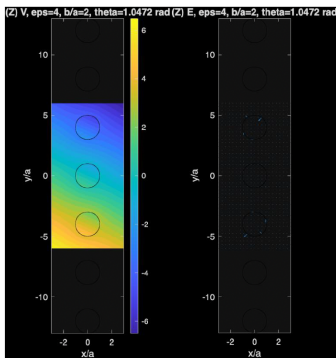
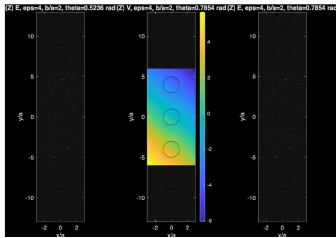
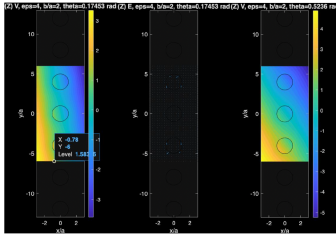
In the following plots, the electric and potential fields in the X-Y plane are depicted for 3 materials with permittivities  $\varepsilon = 2, 4, 10$ , as well as for perfectly conducting cylinders. The assumptions are:  $b = 2a$  and  $\theta = 0$ .



As we observe from the graphs above, for  $\theta = 0$ , the field is horizontal. By increasing the permittivity  $\varepsilon$ , i.e., for a non-PEC (Perfect Electric Conductor) material, the external term  $A_x = \frac{\xi}{1 + \xi S} E_0$  approaches the PEC limit ( $\xi \rightarrow 1$ ), and the field slips around the cylinders with increasingly stronger distortion.

## VII. PLOTTING OF THE ELECTRIC AND POTENTIAL FIELDS IN THE X-Y PLANE (2)

In the following plots, the electric and potential fields in the X-Y plane are depicted for angles  $\theta = 10^\circ, 30^\circ, 45^\circ, 60^\circ$ . The assumptions are:  $b = 2a$  and  $\varepsilon = 4$ .



As can be seen from the plots above, the factor  $S = \frac{a^2 \pi^2}{b^2 12}$  controls all the non-locality. We observe that for small  $\frac{b}{a}$ , due to the inversely proportional relationship of  $S$  with  $\frac{b}{a}$ , we have: when  $\frac{b}{a} = 1.1$ ,  $S$  is large, hence there is strong interaction. For sparser arrays, i.e., for  $\frac{b}{a} = 1.5, 2.5$ , and  $4$ ,  $S$  is small, so we revert close to the single cylinder solution.

#### REFERENCES

- [1] I. A. Roumeliotis and I. Tsalamengas, *Electromagnetic Fields, Volume II*, 2nd ed. Tziolas Publications, Thessaloniki, 2010.
- [2] N. K. Uzunoglu, *Basic Principles of Electromagnetism* (in Greek), Symmetria Publications, Athens, 2004.
- [3] I. A. Roumeliotis, *Electromagnetic Fields, Volume I* (in Greek), 2nd ed. Tziolas Publications, Thessaloniki, 2007.

As we observe from the plots above, the projection along the y-axis excites the enhanced branch  $A_y = \frac{\xi}{1-\xi S} E_{0y}$ . As the angle  $\theta$  increases, the equipotential curves tilt and a stronger deflection appears along the direction of the array.

#### VIII. PLOTTING OF THE ELECTRIC AND POTENTIAL FIELDS IN THE X-Y PLANE (3)

In the following plots, the electric and potential fields in the X-Y plane are depicted for periods  $b = 1.1a, 1.5a, 2.5a, 4a$ . The assumptions are:  $\theta = \pi/4$  and  $\varepsilon = 10$ .

